LETTER

Taxonomic and nutrient controls on phytoplankton iron quotas in the ocean

Benjamin S. Twining [ID],[1]* Olga Antipova,[2] P. Dreux Chappell [ID],[3] Natalie R. Cohen,[4,a] Jeremy E. Jacquot,[1] Elizabeth L. Mann,[1,b] Adrian Marchetti [ID],[4] Daniel C. Ohnemus,[1,a] Sara Rauschenberg,[1] Alessandro Tagliabue [ID][5]

[1]Bigelow Laboratory for Ocean Sciences, East Boothbay, Maine; [2]X-ray Science Division, Advanced Photon Source, Argonne National Laboratory, Lemont, Illinois; [3]Department of Ocean, Earth and Atmospheric Sciences, Old Dominion University, Norfolk, Virginia; [4]Department of Marine Sciences, University of North Carolina at Chapel Hill, Chapel Hill, North Carolina; [5]School of Environmental Sciences, University of Liverpool, Liverpool, UK

Scientific Significance Statement

Iron availability controls phytoplankton growth and community composition in large regions of the ocean, affecting ocean carbon uptake and biomass of higher trophic levels. It is important to constrain the amount of iron both required and actually accumulated by phytoplankton in order to accurately model and predict global ocean productivity, but there are very few direct measurements of phytoplankton iron contents in natural systems. We measured iron in phytoplankton cells collected across gradients of iron and nitrogen in the Pacific Ocean, finding that co-occurring phytoplankton can accumulate significantly more iron than predicted by laboratory experiments used to parameterize most ocean biogeochemical models. These differences are likely caused by colimitation by other nutrients such as nitrogen, as well as differences in phytoplankton ability to store iron.

Abstract

Phytoplankton iron contents (i.e., quotas) directly link biogeochemical cycles of iron and carbon and drive patterns of nutrient limitation, recycling, and export. Ocean biogeochemical models typically assume that iron quotas are either static or controlled by dissolved iron availability. We measured iron quotas in phytoplankton communities across nutrient gradients in the Pacific Ocean and found that quotas diverged significantly in

---

taxon-specific ways from laboratory-derived predictions. Iron quotas varied 40-fold across nutrient gradients, and nitrogen-limitation allowed diatoms to accumulate fivefold more iron than co-occurring flagellates even under low iron availability. Modeling indicates such "luxury" uptake is common in large regions of the low-iron Pacific Ocean. Among diatoms, both pennate and centric genera accumulated luxury iron, but the cosmopolitan pennate genus *Pseudo-nitzschia* maintained iron quotas 10-fold higher than co-occurring centric diatoms, likely due to enhanced iron storage. Biogeochemical models should account for taxonomic and macronutrient controls on phytoplankton iron quotas.

Iron is an essential nutrient for marine phytoplankton, and its scarcity regulates their activity over large areas of the world ocean. Phytoplankton biomass directly connects the biogeochemical cycles of iron and carbon in the ocean, and its elemental stoichiometry impacts nutrient limitation patterns and the ocean carbon cycle (Boyd et al. 2007; Moore et al. 2013). The biomass-normalized iron content of phytoplankton, typically expressed as Fe/C ratios (i.e., quotas), can vary more than 100-fold in cultured species (Sunda and Huntsman 1995; Marchetti and Maldonado 2016)—far more than ratios of the macronutrients nitrogen and phosphorus. Availability of dissolved Fe (dFe) has been shown to place a primary control on iron quotas (Sunda and Huntsman 1995), but taxa are known to differ in their iron requirements (Sunda et al. 1991; Quigg et al. 2003; Marchetti et al. 2006). Indeed, iron quotas of different diatoms grown under identical conditions in laboratory experiments can vary 10-fold (Ho et al. 2003). Irradiance (Sunda and Huntsman 1997), nitrogen availability (Maldonado and Price 1996), and cellular growth rates (Cullen et al. 2003) are also known to influence iron contents, and these factors vary dynamically in the ocean.

The covariation of abiotic and biological factors across gradients in the ocean presents a challenge for understanding physiological responses to environmental gradients. Iron and nitrogen concentrations typically decrease at different rates moving offshore in upwelling systems (Johnson et al. 1997), resulting in a cascade of nutrient limitation regimes (Fig. 1a). Phytoplankton community composition also shifts over these gradients, with larger phytoplankton (e.g., diatoms) typically being replaced by smaller flagellates and cyanobacteria in offshore waters (Longhurst 2007). Further, diatoms isolated from low-nutrient environments display lower minimum iron quotas than coastal diatoms (Sunda et al. 1991; Marchetti et al. 2006; Strzepek et al. 2011), as do nanoflagellates (Sunda and Huntsman 1995; Botebol et al. 2017). It is thus likely that species competition limits the full expression of physiological plasticity of quotas in natural communities. The emergent community Fe/C ratios that result from both cellular physiology and community composition (Fig. 1a) will drive patterns of nutrient recycling and export (Boyd et al. 2007), but the interplay between potential controls on iron quotas is poorly understood.

Global ocean biogeochemistry models account for phytoplankton Fe/C in different ways. Some impose fixed values and derive iron uptake from carbon fixation rates, some explicitly represent the parallel accumulation of iron and carbon, and others are underpinned by empirical relationships based on iron availability (Tagliabue et al. 2016). Most models (e.g., Moore et al. 2004; Stock et al. 2014; Aumont et al. 2015) use results from laboratory culturing studies that measured iron accumulation while varying iron availability to ground truth their parameterizations (Buitenhuis and Geider 2010). These laboratory studies generally show minimum Fe/C of ≤ 2 μmol mol^{-1} C, increasing 10- to 100-fold in response to additional dFe (Sunda et al. 1991; Sunda and Huntsman 1995; Strzepek et al. 2011) (Fig. 2a). However, cells growing at suboptimal concentrations have lower growth rates (Fig. 2b) and would likely be outcompeted and replaced by other, faster-growing taxa in natural environments. Each phytoplankton taxa thus has an *optimal iron quota* (Fe/C$_{opt}$) that represents the minimum iron content needed to maintain its maximum growth rate (Fig. 2c). Quotas of mixed phytoplankton communities in the ocean should be expected to approach Fe/C$_{opt}$ rather than the minimum Fe/C for a given dFe (Fig. 2d). Additionally, most laboratory culturing studies determine Fe/C in phytoplankton grown with excess macronutrients (typically NO_3), which is rarely the situation in natural communities outside of high-nitrate, low chlorophyll (HNLC) regions (Browning et al. 2017).

To examine the responses of iron quotas in unique taxonomic groups to nutrient gradients in the ocean, we measured the iron quotas of individual diatom and nanoflagellate cells collected during four research cruises in the eastern Pacific Ocean (Fig. 1b). The dissolved and particulate iron, nitrate, and phytoplankton biomass at the 16 stations sampled span order-of-magnitude concentration gradients, resulting in a 100-fold variation in dissolved NO_3/Fe (Supporting Information Table S1). Additionally, iron addition and removal incubations were conducted at four stations within both coastal and offshore waters to determine luxury iron uptake and iron storage capacities in representative taxa of pennate and centric diatoms. Potential drivers of luxury uptake, as well as the predicted occurrence of luxury uptake in open ocean phytoplankton more broadly, were explored with the PISCES global ocean model, which explicitly represents iron uptake in a relatively detailed manner.

Methods

Samples were collected during expeditions to the eastern tropical South Pacific (US GEOTRACES EPZT cruise), the
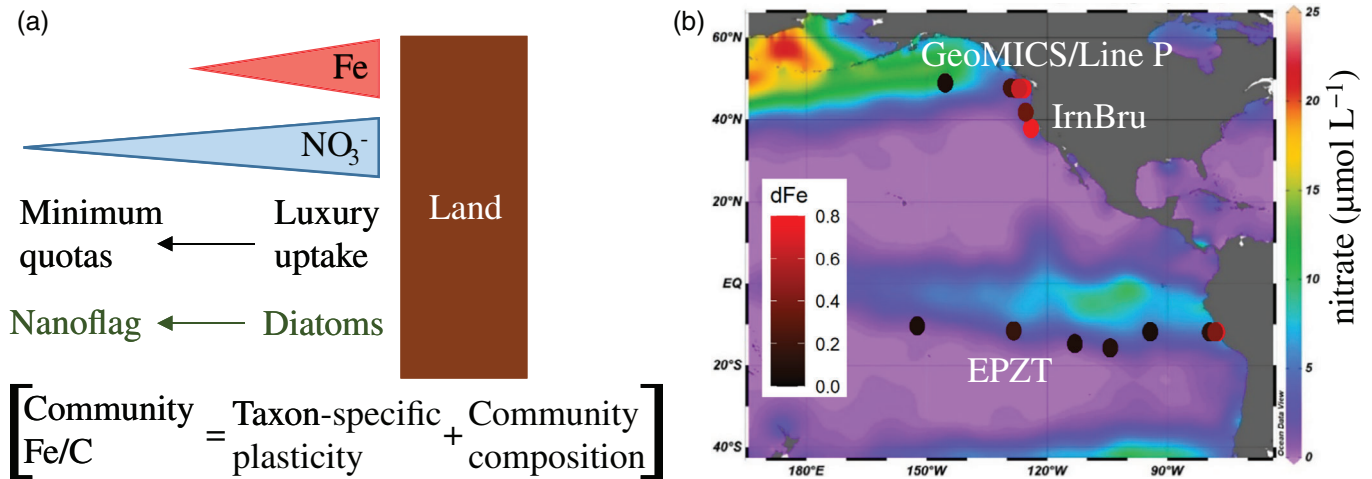
Fig. 1. (**a**) Schematic of factors influencing community Fe/C across ocean nutrient gradients. (**b**) Location of study stations, showing dissolved iron (dFe; symbol color, nmol L^{-1}) overlaid on surface nitrate climatology (μmol L^{-1}, from World Ocean Atlas 2013).

California Upwelling Zone (IRNBRU cruise between Monterey, California and coast of southern Oregon), and two cruises along Line P from Vancouver Island to the subarctic northeast Pacific (GeoMICS cruise in 2012; Line P cruise in 2015). All station locations are provided in Supporting Information Table S1, along with the number and types of samples collected at each station. Each cruise sampled across significant gradients in macronutrient and micronutrient availability. In addition, deckboard bottle incubations in which dFe availability was manipulated were performed on IRNBRU and Line P cruises. Methods specific to each cruise are described in the Supporting Information, and data are available through the Biological and Chemical Oceanography Data Management Office (Twining 2016*a*,2016*b*, 2020*a*,2020*b*; Twining et al. 2016*a*,2016*b*).

Phytoplankton cells were collected from the upper mixed layer (typically 20–25 m) and, in some cases also the subsurface chlorophyll maximum, using trace-metal clean bottles. Samples were prepared for synchrotron X-ray fluorescence (SXRF) analysis (Supporting Information Fig. S1) following protocols described in Twining et al. (2015) and in the Supporting Information. Cellular metals were analyzed with the 2-ID-E microprobe beamline at the Advanced Photon Source, Argonne National Laboratory. Incident beam energy was set at 10 keV to enable the excitation of K_α fluorescence for elements ranging in atomic mass from Si to Zn. Cells were imaged using 2D raster scans with pixel step sizes of 0.3–0.5 μm. Element quantification was performed by averaging the spectra from pixels representing the cells of interest. Concentrations were calculated based on conversion factors obtained from traceable thin-film standards. Cellular C was calculated from cell biovolume, estimated from microscopy. Cells were identified based on cell appearance in light micrographs.

Total and labile particulate metal concentrations were measured following GEOTRACES protocols as described in detail elsewhere (Twining et al. 2015). Briefly, several liters of seawater from each depth were passed through 0.45-μm pore-size Supor polyethersulfone filters to collect particles. Filters were dried and stored frozen until being solubilized with either a mixture of strong acids or a mixture of weak acid and reductant to access total and chemically labile fractions, respectively. Digests were analyzed using a Thermo Element2 HR-ICP-MS equipped with a quartz nebulizer, cyclonic spray chamber, and nickel cones. Element quantification was performed using external calibration curves, and certified reference materials were used to assess recoveries.

Iron addition and removal incubation experiments used to assess iron quota plasticity and luxury uptake are described elsewhere (Cohen et al. 2017; Lampe et al. 2018). Dates, locations, and initial conditions are summarized in Supporting Information Table S2. Briefly, surface seawater was collected using a trace metal clean sampling system into 10-liter cubitainers. Triplicate treatments consisted of 5 nmol L^{-1} of FeCl$_3$, 200 nmol L^{-1} desferroxamine B, and an unamended control. Cubitainers were placed on deck in flow-through incubators with neutral density screening to simulate near-ambient temperature and irradiance. The experimental duration was 24–96 h, with time points varying depending on location. *Chaetoceros* and *Pseudo-nitzschia* cells were collected from each treatment (when present) and analyzed with SXRF.

The PISCES global ocean biogeochemistry model was used to explore nutrient limitation patterns and phytoplankton iron physiology along the EPZT transect. PISCES includes two phytoplankton functional types (diatoms and nanoflagellates), two zooplankton (micro- and mesozooplankton), two particle size classes, particulate biogenic silica, calcium carbonate, five nutrients (nitrate, phosphate, silicic acid, iron, and ammonium), the
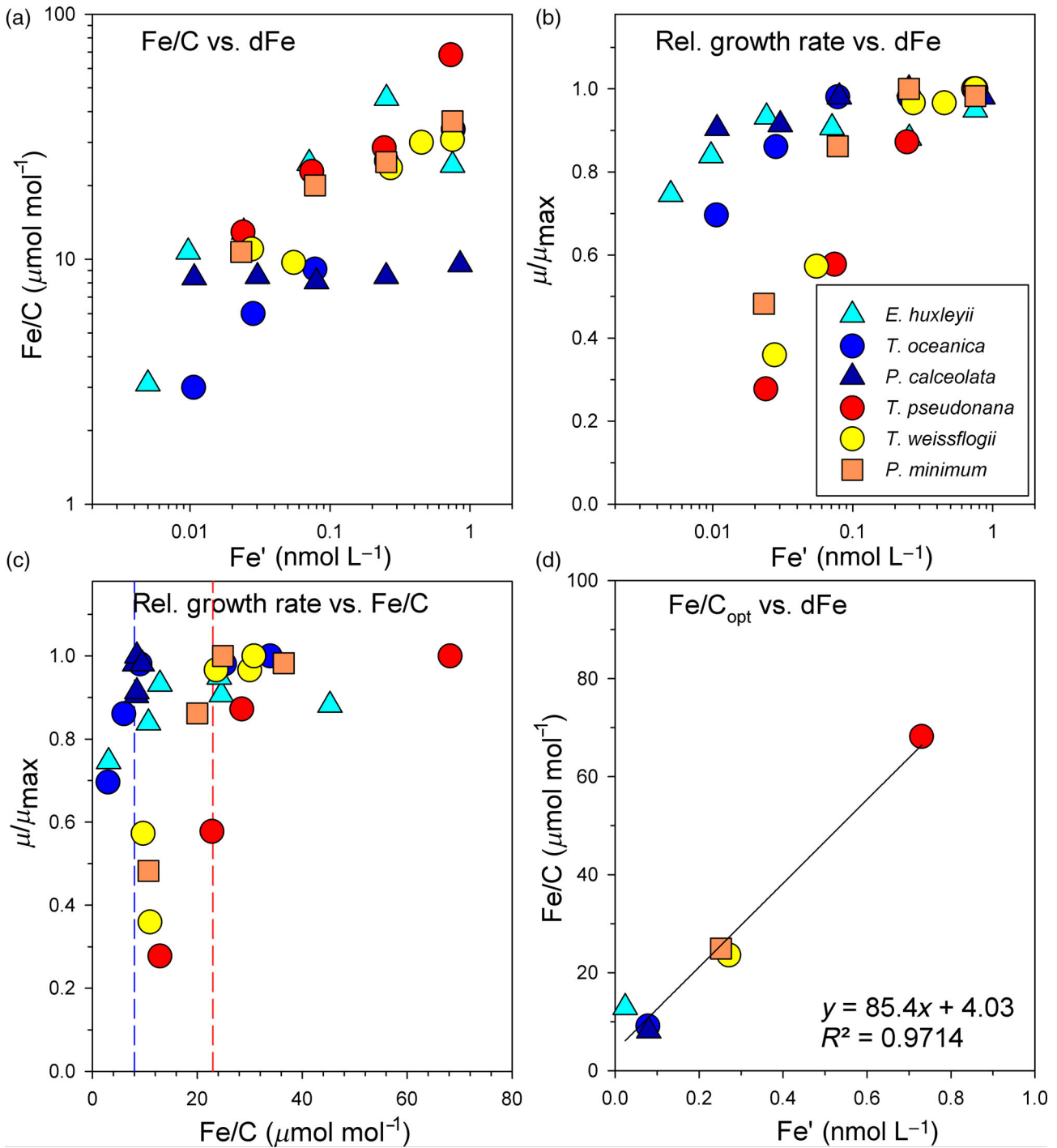
Fig. 2. Responses of six phytoplankton species to iron availability (adapted from Sunda and Huntsman 1995). Symbol color indicates coastal (warm/red shades) or oceanic (cool/blue shades) taxon, and symbol shape indicates diatom (circle), nanoflagellate (triangle), or dinoflagellate (square). (**a**) Iron quota vs. Fe' (sum of inorganic dissolved iron species). (**b**) Relative growth rate (normalized to μ_{max}) vs. Fe'. (**c**) Relative growth rate vs. iron quota. Dashed lines highlight approximate iron quotas when growth rates drop below max levels. (**d**) Optimum iron quota (FeC$_{opt}$: minimum iron quota to achieve max growth rate) vs. Fe'.

full carbon system, oxygen, nitrogen fixation, denitrification, and anammox (Aumont et al. 2015). The PISCES iron cycle is complex, representing a range of sources and explicitly representing phytoplankton iron uptake in response to changing iron availability, iron limitation, and an assumed maximum quota (Tagliabue et al. 2020). The iron quotas are an

emergent feature of the model resulting from iron and carbon assimilation rates. We investigated iron quotas and their drivers in the South Pacific using the standard configuration of the model and an addition experiment where diatoms were not allowed to access the ammonium pool (referred to as "NH4 expt" in Supporting Information Fig. S3).

Results and discussion

Phytoplankton community responses to gradients in iron and nitrogen concentrations

In the eastern tropical South Pacific Ocean, nitrate and iron concentrations decreased approximately 20-fold from productive coastal waters over the shelf to oligotrophic waters at the edge of the subtropical gyre (Fig. 3). Along the onshore-to-offshore transect, iron concentrations declined rapidly, with dFe decreasing to below 0.2 nmol L^{-1} within 223 km from the coast. In contrast, nitrate remained above 5 μmol L^{-1} for an additional approximately 2000 km, resulting in HNLC-like conditions in the middle of the transect (NO_3/Fe: 188 μmol $nmol^{-1}$). Across this gradient, phytoplankton biomass (based on chlorophyll *a* [Chl *a*] as a proxy) declined 27-fold (Fig. 3b), in step with dFe rather than nitrate (r^2 for linear regressions of Chl vs. dFe or nitrate were 0.91 and 0.39, respectively). Phytoplankton community composition also shifted, with diatoms and other larger phytoplankton replaced by nanoflagellates and picophytoplankton moving offshore (Fig. 3b). The decrease in diatoms corresponded more closely with the decrease in nitrate rather than dFe (Fig. 3b), suggesting that iron availability constrains overall phytoplankton biomass while competition for
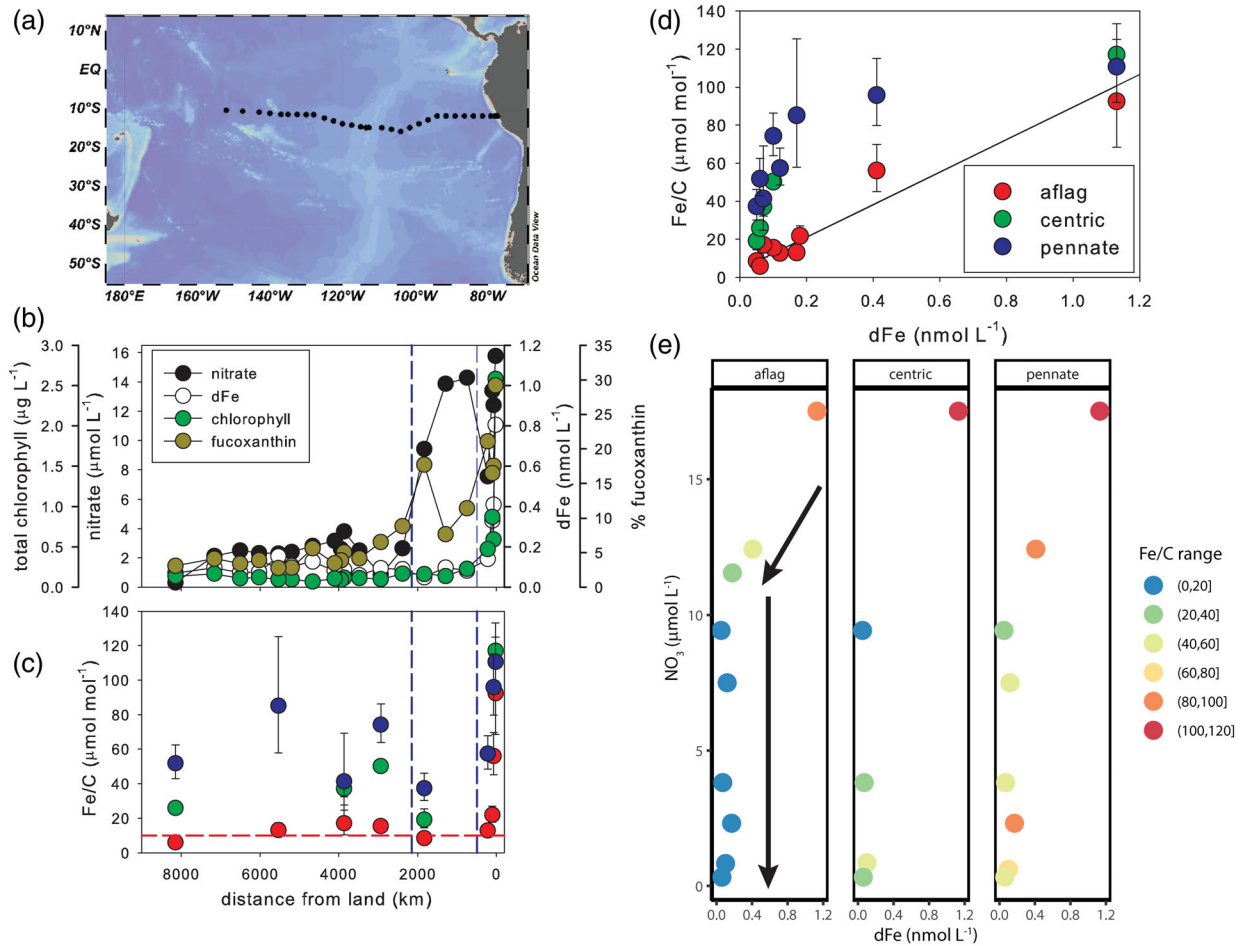
Fig. 3. Response of iron quotas to nutrient gradients in the South Pacific Ocean. (**a**) Location of stations on EPZT cruise, plotted over bathymetry. (**b**) Phytoplankton abundance (total Chl *a*), nitrate, dFe, and relative diatom abundance (% fucoxanthin, a pigment proxy for diatoms) across the onshore-offshore gradient. Data are means of upper 50 m at each station. Dashed blue lines delineate putative coastal, HNLC, and oligotrophic regions (Boiteau et al. 2016). (**c**) Taxon-specific Fe quotas (geometric means ± SE) as a function of location. Dashed red line indicates the optimal Fe/C estimated for open-ocean phytoplankton under low dFe (see text for details). Symbol colors are as indicated in panel (**d**) legend: red—autotrophic flagellates (aflag); green—centric diatoms (centric); blue—pennate diatoms (pennate). (**d**) Taxon-specific Fe quotas as a function of dFe. Also plotted is predicted FeC_{opt} (see text for details). (**e**) Response of taxon-specific Fe quotas to gradients in ambient nitrate and dFe. Symbol color indicates Fe/C (μmol mol^{-1}). Arrows indicate direction of cruise track, moving from shelf westward into the gyre.

nitrate, in addition to Fe, influences community composition. Studies in the eastern equatorial Pacific support that diatoms are primarily growing on nitrate and thus particularly sensitive to its availability in the upper ocean (Price et al. 1994; Parker et al. 2011). The PISCES model captures well the observed gradients in nutrients and phytoplankton community in this region (Supporting Information Fig. S2).

Iron quotas of diatoms and nanoflagellates responded differently to these nutrient gradients, suggesting they are controlled by different factors. Nanoflagellate Fe/C dropped in lock-step with dFe, with iron quotas decreasing from 92 μmol mol^{-1} over the shelf to approximately 13 μmol mol^{-1} in low-Fe waters (Fig. 3c). Nanoflagellate Fe/C remained around 10 μmol mol^{-1} further offshore, and average flagellate iron quotas closely followed predicted Fe/C$_{opt}$ across the section (Fig. 3d). In contrast, iron quotas of diatoms decreased offshore but remained twofold to fivefold above those measured in flagellates and fourfold to sixfold above predicted Fe/C$_{opt}$ (Fig. 3d). While diatom Fe/C appears to saturate around 0.4 nmol L^{-1} as nanoflagellate Fe/C continues to increase, we hypothesize that this behavior is caused by differential nitrogen limitation (see discussion below) rather than unique iron uptake functions for diatoms and flagellates. Despite these elevated iron quotas, diatom abundance decreased to less than 5% of the overall phytoplankton community offshore (Fig. 3b), while nanoflagellate taxa comprised 30–50% of the community, based on diagnostic accessory pigments (Supporting Information Table S1). Higher Fe/C in diatoms is unlikely to be driven by Fe associated with the frustule, which has been shown to comprise < 5% of cellular Fe (Ellwood and Hunter 2000). The PISCES model also predicts higher iron quotas both nearshore and far offshore, with the lowest quotas also found in the iron-limited HNLC region (Fig. 4c). The model indicates this pattern results from a succession of different nutrient regimes moving offshore, with systematic changes in iron and carbon assimilation moving from nutrient-replete to iron-limited to nitrogen-limited systems (Fig. 4a,b). However, PISCES does not reproduce the observed bifurcation between diatom and nanoflagellate quotas offshore, with both groups responding similarly in the model (Fig. 4c).

The low abundance but elevated iron contents of diatoms offshore suggests that nitrogen limitation of growth allows diatoms to accumulate iron above the predicted Fe/C$_{opt}$. The lowest iron quotas for both diatoms and flagellates were measured in waters still replete with nitrate but deficient in iron (Fig. 3e). Diatom iron quotas then increase further offshore as nitrate concentrations continue to decline, even as dFe remains very low (< 0.2 nmol L^{-1}). Lower rates of diatom cell division (suggested by lower abundances) due to nitrogen limitation would enable iron to accumulate to higher levels in cells even under very low dFe. Such a "growth rate dilution" effect has been invoked previously to explain changes in metal quotas under changing growth regimes (Kudo et al. 1996; Cullen et al. 2003). This mechanism is present in the PISCES model, which shows a sharper decline in carbon fixation than iron uptake for both phytoplankton groups moving into the nitrogen limited offshore region (Fig. 4a,b). Interestingly, additional experiments with our model, in which diatoms were made completely reliant on nitrate as a nitrogen source (consistent with local observations; Price et al. 1994; Parker et al. 2011), caused diatom and nanoflagellate iron quotas to increase and decrease, respectively, more closely matching our measurements in the nitrogen-limited offshore region (Fig. 4c). This highlights the role of nitrogen, and particularly the balance between nitrate and ammonium, in shaping iron quotas in nitrogen deplete systems. As diatom iron quotas exceeded nanoflagellate quotas at both Fe- and N-limited stations, these differences may be driven by a combination of slower growth and luxury iron uptake.

More broadly, our model experiments indicate that the overconsumption of iron, relative to carbon assimilation, by diatoms in nitrate-poor waters is widespread in low-macronutrient Pacific surface waters (Fig. 4d). This suggests that diatom Fe/C in the nitrogen-deplete global ocean are poorly represented by laboratory culture work conducted under nitrogen-replete conditions. Indeed, measurements of bulk particulate Fe/C in the Pacific Ocean show levels (ca. 50 μmol mol^{-1}) well above those predicted for phytoplankton from laboratory-derived Fe/C$_{opt}$ (Supporting Information Tables S1, S3). As diatoms are more likely to sink and drive biogeochemical fluxes (Buesseler 1998), increased diatom Fe/C in the nitrate-deplete, low-iron oligotrophic Pacific Ocean will strongly affect upper ocean recycling and export of iron and carbon.

## Taxon-specific responses of diatoms to an iron gradient

Given the surprising behavior of diatom iron quotas in the South Pacific Ocean and growing knowledge about diverse iron physiologies of diatom classes (Groussman et al. 2015; Marchetti and Maldonado 2016), we further investigated the iron quotas of individual centric and pennate diatom taxa across a similar nutrient gradient in the sub-Arctic North Pacific Ocean (GeoMICS/Line P transect; Fig. 5a). As in the South Pacific, concentrations of dFe and nitrate decreased significantly (4- and 26-fold, respectively) from onshore to offshore, along with diatom and overall phytoplankton biomass (Fig. 5b). Coastal species of both centric (e.g., *Guinardia* sp., *Thalassiosira pacifica*) and pennate (e.g., *Pseudo-nitzschia pungens*) diatoms were replaced by oceanic species (e.g., *Thalassiosira oceanica* and *Pseudo-nitzschia granii*, respectively) offshore (Chappell et al. 2019) (Fig. 5d). However, iron quotas in centrics and pennates responded differently to these nutrient gradients. Average centric Fe/C decreased threefold, from 36 μmol mol^{-1} nearshore to 12 μmol mol^{-1} offshore, close to predicted Fe/C$_{opt}$ (Fig. 5c). In contrast, average pennate diatom Fe/C were at least twice those of centric diatoms at all stations and nearly sevenfold higher at the furthest offshore station.

Examining the behavior of individual diatom taxa across the nutrient gradient reveals the interplay of physiological acclimation and community adaptation (i.e., species succession). Iron


quotas of the coastal diatoms *Chaetoceros* sp., *Guinardia* sp., and *Cylindrotheca* sp. were plastic and sensitive to dFe, decreasing approximately fourfold within each taxon as dFe decreased offshore (Fig. 5d, Supporting Information Fig. S4). Average Fe/C of these taxa co-occurring at the nearshore station spanned 10-fold (24–236 μmol mol^{-1}), demonstrating the strong influence of taxonomy on biogeochemistry. Smaller centric diatom quotas displayed less plasticity, with average quotas spanning only fourfold over the entire transect. In contrast, *Pseudo-nitzschia* species exhibited unique behavior, maintaining iron quotas of 50–84 μmol mol^{-1} across the entire transect, even as the dominant species shifted from *P. pungens* to *P. granii*. Indeed, *Pseudo-nitzschia* iron quotas appeared to be nearly insensitive to Fe availability. Given the relative dominance of *Pseudo-nitzschia* in the diatom community offshore (Fig. 5d) (Chappell et al. 2019), the ability to acquire and/or store iron appears to provide members of this genus with a competitive advantage. These data demonstrate the biogeochemical impact of niche partitioning, with diverse phytoplankton groups having distinct iron strategies and using external iron sources differently, even as they occupy the same system.

Enhanced storage capability supports elevated diatom iron quotas

A series of incubation experiments conducted with the diatom communities in the North Pacific suggest that enhanced iron storage capabilities underpin *Pseudo-nitzschia*'s unique ability to maintain elevated quotas. A greater ability to store excess iron, obtained either from lowered growth rate dilution or a pulsed iron input, should increase competitiveness, and the unique iron storage capabilities of *Pseudo-nitzschia* have been measured in culture (Marchetti et al. 2009). We compared iron quotas of co-occurring *Pseudo-nitzschia* sp. and *Chaetoceros* sp. in natural communities across a 10-fold range of iron availabilities. *Chaetoceros* were > 10-fold more abundant than *Pseudo-nitzschia* at the highest iron conditions (3.5 nmol L^{-1}), and ambient *Chaetoceros* accumulated Fe/C to maximum levels (150 μmol mol^{-1}), fivefold above quotas in cells collected from the same station and subsequently starved of iron (Fig. 6). At lower ambient dFe (1.0 nmol L^{-1}), *Pseudo-nitzschia* became more abundant than *Chaetoceros* and maintained iron quotas at maximum levels (ca. 50 μmol Fe/mol C, also fivefold above iron-
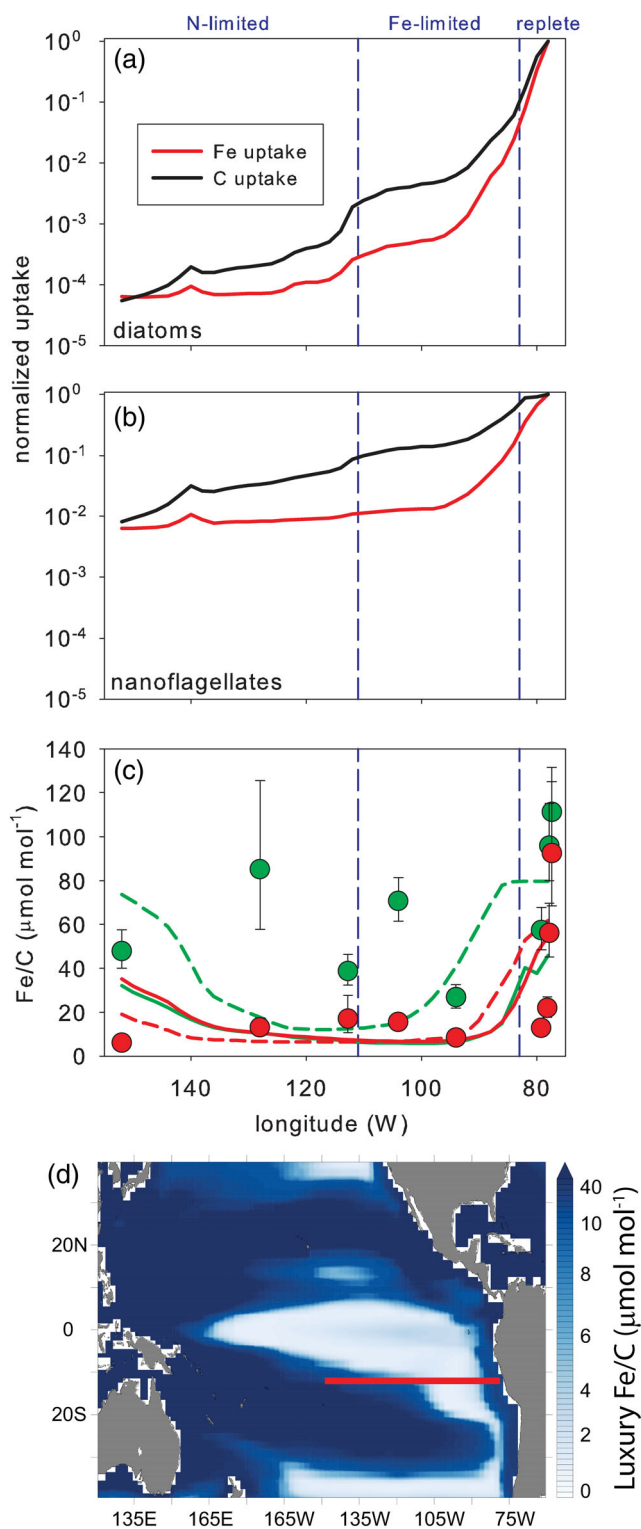
Fig. 4. Calculated iron and carbon uptake rates (mol m^{-3} s^{-1}) for (**a**) diatoms and (**b**) nanoflagellates, as calculated by the PISCES model and normalized to maximum uptake rates on the eastern side of the EPZT transect. Dashed vertical blue lines indicate regions predicted by PISCES model to be limited by N, Fe, or neither (replete). (**c**) Cellular Fe/C in the eastern tropical South Pacific calculated by PISCES model for standard run (solid lines) and NH4 run (dashed lines, see text for details). Iron quotas measured with SXRF are shown as circles (geometric mean ± SE). The underlying components of the predicted Fe/C for each group are shown in Supporting Information Fig. S3. (**d**) Distribution of luxury iron accumulated by N-limited diatoms in the Pacific Ocean predicted by PISCES model (control run). The EPZT section is marked with a red line.
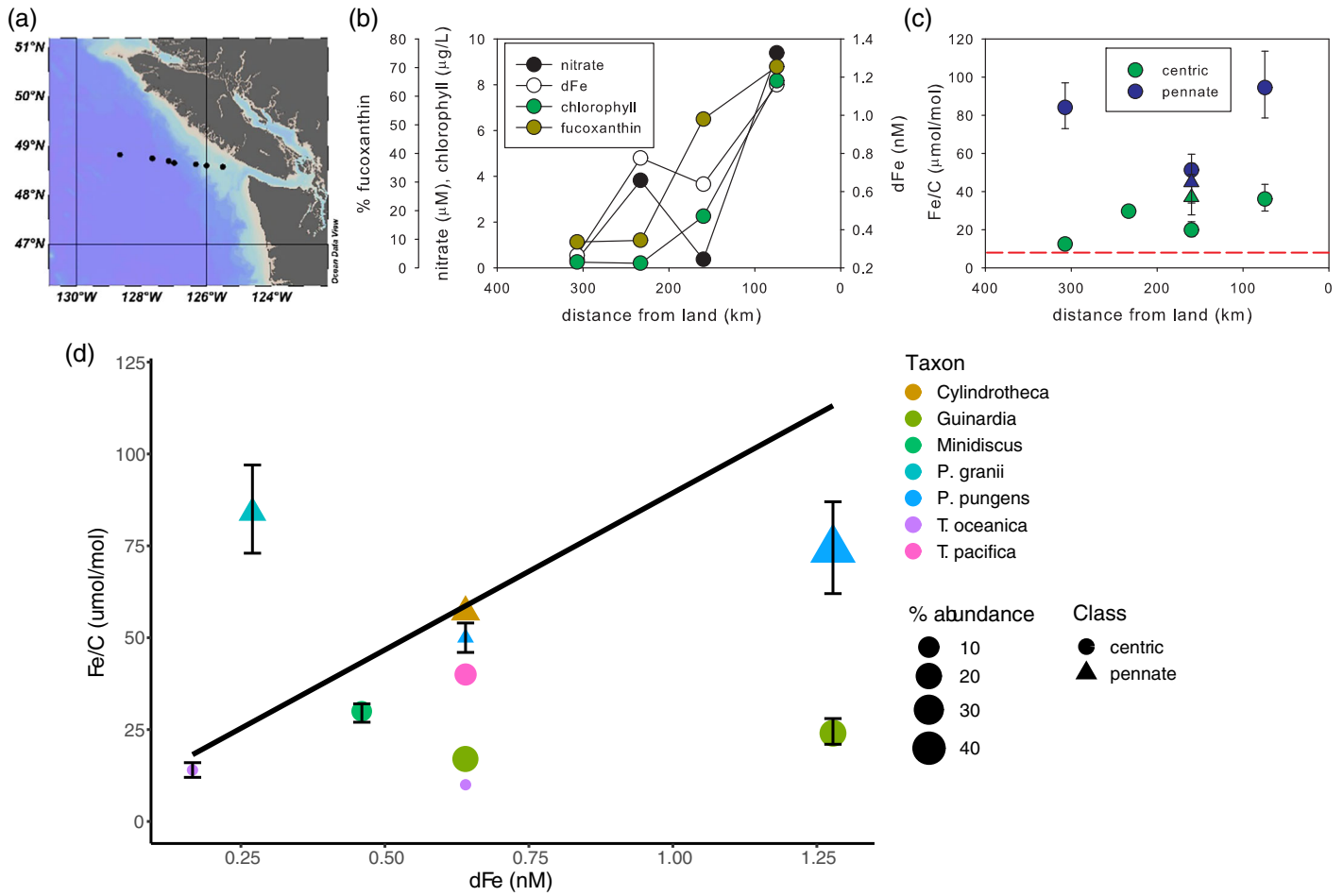
Fig. 5. (**a**) Map of stations along GeoMICS transect. (**b**) Nitrate, dFe, Chl *a*, and diatom abundance (% fucoxanthin) across Line P in the North Pacific Ocean. Data are means of upper 50 m at each station. (**c**) Average centric and pennate diatom iron quotas across the transect. Circles are data from May 2012 GeoMICS cruise, and triangles are data from June 2015 Line P cruise. Red line indicates the minimum Fe/C$_{opt}$ estimated for open-ocean phytoplankton under low dFe (see text for details). (**d**) Average iron quotas of individual diatom taxa from GeoMICS cruise as a function of dFe. Black symbols show predicted Fe/C$_{opt}$. Symbol size indicates taxon abundance (18S reads normalized to total diatom reads). Only taxa with 18S gene abundance > 1% of total diatom reads are shown. Diatom abundance data are summarized in Supporting Information Table S4, and the behaviors of individual taxa are broken out in Supporting Information Fig. S4.

starved cells). With dFe further reduced (0.64 nmol⁻¹), *Pseudo-nitzschia* was able to store iron at maximum levels while *Chaetoceros* cells could accumulate iron to only 70% of maximum levels. Furthermore, *Pseudo-nitzschia* were able to reduce minimum quotas to half of *Chaetoceros* levels (10 μmol mol⁻¹ compared to 18 μmol mol⁻¹, respectively), providing an additional competitive advantage (Marchetti et al. 2006). At the lowest dFe incubation (Station Papa; 0.05 nmol L⁻¹), *Pseudo-nitzschia* luxury storage capacity doubled following iron addition, in-line with ferritin expression (Lampe et al. 2018), and cells were able to maintain quotas threefold above minimum levels even in the absence of added iron (Fig. 6). In contrast, *Chaetoceros* were unable to achieve adequate cell concentrations to be analyzed.

Implications for ocean ecology and biogeochemistry

Our results show that phytoplankton respond to nutrient gradients by altering their iron quotas in taxon-specific ways, and importantly, that certain taxa are able to accumulate luxury iron more than others. We have identified that nitrogen availability also influences iron quotas. Differences in the accumulation of iron among phytoplankton taxa will impact ecological competition, as those taxa able to store iron following sporadic inputs will be able to outcompete other groups when iron is subsequently depleted (Marchetti et al. 2009). This likely explains the dominant response of *Pseudo-nitzschia* to experimental iron inputs (De Baar et al. 2005). Excess cellular iron within diatoms in the Pacific gyre would also allow them to respond favorably to pulsed inputs of nitrogen. Iron
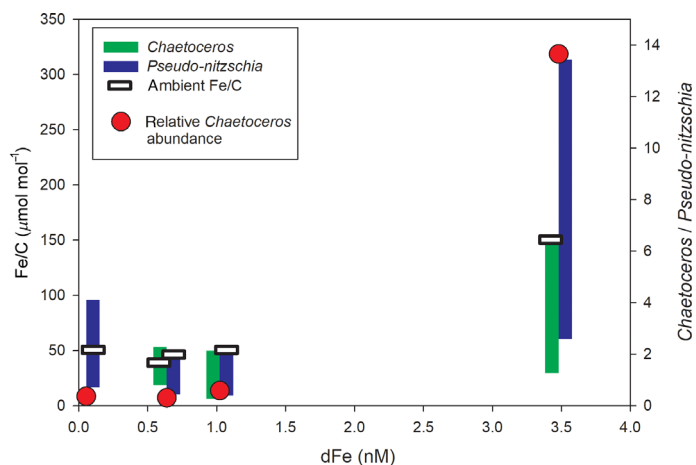
Fig. 6. Luxury iron uptake and storage in natural communities of *Chaetoceros* and *Pseudo-nitzschia* in the California Current System and along Line P. The range of maximum and minimum observed average iron quotas in *Chaetoceros* and *Pseudo-nitzschia* populations from incubation experiments are plotted as a function of initial dissolved iron at the incubation stations. The white bars at each station show Fe/C measured in the initial population (three high-iron incubations) or in the unamended control treatment when initial population was not analyzed (lowest-iron incubation). Also plotted is the relative abundance of *Chaetoceros* and *Pseudo-nitzschia* based on metatranscriptomic gene abundance (Lampe et al. 2018). The responses of group Fe/C across all incubation timepoints are shown in Supporting Information Fig. S5.

uptake and storage by phytoplankton are predicted to impact productivity of higher trophic levels in the ocean, with models suggesting that changes to iron accumulation by phytoplankton in the equatorial Pacific will impact upper trophic levels in the coming century (Tagliabue et al. 2020). Our ability to predict responses of marine ecosystems to nutrient inputs thus depends on our understanding of taxon-specific nutrient acquisition and storage capabilities, which will be advanced by combining taxon-specific measurements of physiology through "omic approaches with taxon-specific nutrient measurements (e.g., Lampe et al. 2018).

Luxury iron uptake will also impact biogeochemical iron cycling throughout low-nutrient areas. Large regions of the ocean experience macronutrient limitation (Moore et al. 2013), and the resulting accumulation of iron above minimum levels in these areas may increase iron recycling (Richon et al. 2020), retention of iron by phytoplankton communities (Rafter et al. 2017), and potentially intensify nitrogen limitation. Furthermore, future increases in stratification and ensuing macronutrient limitation suggest that departures in iron quotas from laboratory-predicted Fe/C$_{opt}$ will become even more pervasive. These underlying drivers need to be incorporated into both conceptual and numerical models of ocean biogeochemical cycling. To fully understand the importance of biological diversity and physiological dynamics now recognized in ocean phytoplankton, we must directly assess the biogeochemical signals that key members of these communities impart.

References

Aumont, O., C. Ethé, A. Tagliabue, L. Bopp, and M. Gehlen. 2015. PISCES-v2: An ocean biogeochemical model for carbon and ecosystem studies. Geosci. Model Dev. **8**: 2465–2513. doi:10.5194/gmd-8-2465-2015.

Boiteau, R. M., and others. 2016. Siderophore-based microbial adaptations to iron scarcity across the eastern Pacific Ocean. Proc. Natl. Acad. Sci. USA **113**: 14237–14242. doi: 10.1073/pnas.1608594113.

Botebol, H., and others. 2017. Acclimation of a low iron adapted *Ostreococcus* strain to iron limitation through cell biomass lowering. Sci. Rep. **7**: 327. doi: 10.1038/s41598-017-00216-6.

Boyd, P. W., and others. 2007. Mesoscale iron enrichment experiments 1993-2005: Synthesis and future directions. Science **315**: 612–617. doi:10.1126/science.1131669.

Browning, T. J., E. P. Achterberg, I. Rapp, A. Engel, E. M. Bertrand, A. Tagliabue, and C. M. Moore. 2017. Nutrient co-limitation at the boundary of an oceanic gyre. Nature **551**: 242–246. doi:10.1038/nature24063.

Buesseler, K. O. 1998. The decoupling of production and particulate export in the surface ocean. Global Biogeochem. Cycles **12**: 297–310. doi:10.1029/97GB03366.

Buitenhuis, E. T., and R. J. Geider. 2010. A model of phytoplankton acclimation to iron-light colimitation. Limnol. Oceanogr. **55**: 714–724. doi:10.4319/lo.2010.55.2.0714.

Chappell, P. D., E. V. Armbrust, K. A. Barbeau, R. M. Bundy, J. W. Moffett, J. Vedamati, and B. D. Jenkins. 2019. Patterns of diatom diversity correlate with dissolved trace metal concentrations and longitudinal position in the northeast Pacific coastal–offshore transition zone. Mar. Ecol. Prog. Ser. **609**: 69–86. doi:10.3354/meps12810.

Cohen, N. R., and others. 2017. Diatom transcriptional and physiological responses to changes in iron bioavailability across ocean provinces. Front. Mar. Sci. **4**: 360. doi:10.3389/fmars.2017.000360.

Cullen, J. T., Z. Chase, K. H. Coale, S. E. Fitzwater, and R. M. Sherrell. 2003. Effect of iron limitation on the cadmium to phosphorus ratio of natural phytoplankton assemblages from the Southern Ocean. Limnol. Oceanogr. **48**: 1079–1087. doi:10.4319/lo.2003.48.3.1079.

De Baar, H. J. W., and others. 2005. Synthesis of iron fertilization experiments: From the iron age in the age of enlightenment. J. Geophys. Res. Oceans **110**: 1–24.

Ellwood, M. J., and K. A. Hunter. 2000. The incorporation of zinc and iron into the frustule of the marine diatom *Thalassiosira pseudonana*. Limnol. Oceanogr. **45**: 1517–1524. doi:10.4319/lo.2000.45.7.1517.

Groussman, R. D., M. S. Parker, and E. V. Armbrust. 2015. Diversity and evolutionary history of iron metabolism genes in diatoms. PLoS One **10**: e0129081. doi:10.1371/journal.pone.0129081.

Ho, T. Y., A. Quigg, Z. V. Finkel, A. J. Milligan, K. Wyman, P. G. Falkowski, and F. M. M. Morel. 2003. The elemental composition of some marine phytoplankton. J. Phycol. **39**: 1145–1159. doi:10.1111/j.0022-3646.2003.03-090.x.

Johnson, K. S., R. M. Gordon, and K. H. Coale. 1997. What controls dissolved iron concentrations in the world ocean? Mar. Chem. **57**: 137–161. doi:10.1016/S0304-4203(97)00043-1.

Kudo, I., H. Kokubun, and K. Matsunaga. 1996. Chemical fractionation of phosphorus and cadmium in the marine diatom *Phaeodactylum tricornutum*. Mar. Chem. **52**: 221–231. doi:10.1016/0304-4203(95)00086-0.

Lampe, R. H., and others. 2018. Different iron storage strategies among bloom-forming diatoms. Proc. Natl. Acad. Sci. USA **115**: E12275–E12284. doi:10.1073/pnas.1805243115.

Longhurst, A. 2007, *Ecological geography of the sea*, 2nd Edition. Academic Press.

Maldonado, M. T., and N. M. Price. 1996. Influence of N substrate on Fe requirements of marine centric diatoms. Mar. Ecol. Prog. Ser. **141**: 161–172. doi:10.3354/meps141161.

Marchetti, A., M. T. Maldonado, E. S. Lane, and P. J. Harrison. 2006. Iron requirements of the pennate diatom *Pseudo-nitzschia*: Comparison of oceanic (high-nitrate, low-chlorophyll waters) and coastal species. Limnol. Oceanogr. **51**: 2092–2101. doi:10.4319/lo.2006.51.5.2092.

Marchetti, A., and others. 2009. Ferritin is used for iron storage in bloom-forming marine pennate diatoms. Nature **457**: 467–470. doi:10.1038/nature07539.

Marchetti, A., and M. T. Maldonado. 2016. Iron, p. 233–280. *In* M. A. Borowitzka, J. Beardall, and J. A. Raven [eds.], *The physiology of microalgae. Developments in applied phycology*. Springer.

Moore, C. M., and others. 2013. Processes and patterns of oceanic nutrient limitation. Nat. Geosci. **6**: 701–710. doi:10.1038/ngeo1765.

Moore, J. K., S. C. Doney, and K. Lindsay. 2004. Upper ocean ecosystem dynamics and iron cycling in a global three-dimensional model. Global Biogeochem. Cycles **18**: GB4028. doi:10.1029/2004GB002220.

Parker, A. E., F. P. Wilkerson, R. C. Dugdale, A. M. Marchi, V. E. Hogue, M. R. Landry, and A. G. Taylor. 2011. Spatial patterns of nitrogen uptake and phytoplankton in the equatorial upwelling zone (110 degrees W-140 degrees W) during 2004 and 2005. Deep-Sea Res. Part II Top. Stud. Oceanogr. **58**: 417–433. doi:10.1016/j.dsr2.2010.08.013.

Price, N. M., B. A. Ahner, and F. M. M. Morel. 1994. The equatorial Pacific Ocean: Grazer-controlled phytoplankton populations in an iron-limited ecosystem. Limnol. Oceanogr. **39**: 520–534. doi:10.4319/lo.1994.39.3.0520.

Quigg, A., and others. 2003. The evolutionary inheritance of elemental stoichiometry in marine phytoplankton. Nature **425**: 291–294. doi:10.1038/nature01953.

Rafter, P. A., D. M. Sigman, and K. R. M. Mackey. 2017. Recycled iron fuels new production in the eastern equatorial Pacific Ocean. Nat. Commun. **8**: 1100. doi:10.1038/s41467-017-01219-7

Richon, C., O. Aumont, and A. Tagliabue. 2020. Prey stoichiometry drives iron recycling by zooplankton in the global ocean. Front. Mar. Sci. **7**: 451. doi:10.3389/fmars.2020.00451

Stock, C. A., J. P. Dunne, and J. G. John. 2014. Global-scale carbon and energy flows through the marine planktonic food web: An analysis with a coupled physical–biological model. Prog. Oceanogr. **120**: 1–28. doi:10.1016/j.pocean.2013.07.001.

Strzepek, R. F., M. T. Maldonado, K. A. Hunter, R. D. Frew, and P. W. Boyd. 2011. Adaptive strategies by Southern Ocean phytoplankton to lessen iron limitation: Uptake of organically complexed iron and reduced cellular iron requirements. Limnol. Oceanogr. **56**: 1983–2002. doi:10.4319/lo.2011.56.6.1983.

Sunda, W. G., D. G. Swift, and S. A. Huntsman. 1991. Low iron requirement for growth in oceanic phytoplankton. Nature **351**: 55–57. doi:10.1038/351055a0.

Sunda, W. G., and S. A. Huntsman. 1995. Iron uptake and growth limitation in oceanic and coastal phytoplankton. Mar. Chem. **50**: 189–206. doi:10.1016/0304-4203(95)00035-P.

Sunda, W. G., and S. A. Huntsman. 1997. Interrelated influence of iron, light and cell size on marine phytoplankton growth. Nature **390**: 389–392. doi:10.1038/37093.

Tagliabue, A., and others. 2016. How well do global ocean biogeochemistry models simulate dissolved iron distributions? Global Biogeochem. Cycles **30**: 149–174. doi:10.1002/2015GB005289.

Tagliabue, A., and others. 2020. An iron cycle cascade governs the response of equatorial Pacific ecosystems to climate change. Glob. Chang. Biol. **26**: 6168–6179. doi:10.1111/gcb.15316.

Twining, B. S. 2016*a*. Element quotas of individual phytoplankton cells from GEOTRACES-EPZT cruise TN303, 2013. Biological and Chemical Oceanography Data Management Office (BCO-DMO). Version Date 2016-07-19. Available from https://lod.bco-dmo.org/id/dataset/643270. Accessed November 25, 2020.

Twining, B. S. 2016*b*. Particulate data collected on R/V Melville (MV1405, IrnBru) along the California coast in July 2014. Biological and Chemical Oceanography Data Management Office (BCO-DMO). Version Date 2016-10-26. Available from http://lod.bco-dmo.org/id/dataset/663183. Accessed November 25, 2020.

Twining, B. S. 2020*a*. Phytoplankton metal quotas from GeoMICS cruise in NE Pacific Ocean. Biological and Chemical Oceanography Data Management Office (BCO-DMO). Version data 2020-11-25. Available from https://www.bco-dmo.org/project/517510. Accessed November 25, 2020.

Twining, B. S. 2020*b*. Phytoplankton metal quotas from IRNBRU cruise in coastal California upwelling system. Biological and Chemical Oceanography Data Management Office (BCO-DMO). Version date 2020-11-25. Available from https://www.bco-dmo.org/project/527114. Accessed November 25, 2020.

Twining, B. S., S. Rauschenberg, P. L. Morton, and S. Vogt. 2015. Metal contents of phytoplankton and labile particulate material in the North Atlantic Ocean. Prog. Oceanogr. **137**: 261–283. doi:10.1016/j.pocean.2015.07.001.

Twining, B. S., J. W. Moffett, and M. A. Saito. 2016*a*. Trace element concentrations in dissolved and particulate fractions from samples collected by GO-Flo bottles on R/V Thomas G. Thompson cruise TN280 along Line P in the NE Pacific in May 2012 (GeoMICS project). Biological and Chemical Oceanography Data Management Office (BCO-DMO). Version Date 2016-11-16. Available from http://lod.bco-dmo.org/id/dataset/664975. Accessed November 25, 2020.

Twining, B. S., R. M. Sherrell, and C. R. German. 2016*b*. Trace elements in suspended particles from GO-Flo bottles. Biological and Chemical Oceanography Data Management Office (BCO-DMO). Version Date 2016-05-17. Available from http://lod.bco-dmo.org/id/dataset/639847. Accessed November 25, 2020.